

Electronic Nature of Carbonium Ions and Their Silicon Analogues

Caio L. Firme,* O. A. C. Antunes, and Pierre M. Esteves*

Universidade Federal do Rio de Janeiro, Instituto de Química, Avenida Athos da Silveira Ramos, 149, CT Bloco A, Sala 622, Cidade Universitária, Ilha do Fundão, Rio de Janeiro, BR 21941-909, Brazil

Received: November 5, 2007; In Final Form: January 10, 2008

Nonclassical ions or carbonium ions have multi-center bonding from delocalized σ or π electrons. The 2-norbornyl cation, its derivative 6,6-difluoro-2-norbornyl cation, tris-homocyclopropenyl cation, 7-norbornenyl cation, and 4-cyclopentenyl cation and their corresponding silicon analogues were studied in this work. All carbocations have topologically different 3c–2e systems. The magnitude of all delocalization indexes between each atomic pair of the 3c–2e bond can be used to predict homoaromaticity. The silicon analogues have a topologically different 3c–2e bond from their corresponding carbocation.

Introduction

Characterization of the first long-lived alkyl cation (*t*-butyl cation) by Olah^{1,2} represented a turning point in chemistry. Superacids and stable ion conditions have played a decisive role in carbocation chemistry^{3,4} since they afforded carbocations to be observed without unwanted side reactions.^{5,6}

In 1949, Winstein and Trifan⁷ postulated the assistance of σ electron delocalization to account for great rate differences in the acetolysis of *exo*- and *endo*-2-norbornyl brosilates. On the other hand, Brown⁸ attributed these differences to steric effects. Thereafter, heated debates on the nature of the norbornyl cation, called the nonclassical ion controversy, took place.^{8–10} The term nonclassical ions was first used by Roberts and Mazur¹¹ in their pioneering solvolytic studies on cyclobutyl and cyclopropyl-carbinyl derivatives. Experimental evidence^{12,13} indicated that the norbornyl cation had no trivalent carbenium center, which is characteristic of classical ions. Then, the nonclassical nature of the hypercoordinate norbornyl cation, characterized by delocalized σ electrons in three-center–two-electron (3c–2e) bonding, was proved.¹⁴

Crystallographic studies¹⁵ of boron hydrides gave rise to the development of multi-center bonding.^{16,17} The discovery of a significant number of nonclassical ions or carbonium ions showed that carbon hypercoordination is a common phenomenon in carbocation chemistry. The 3c–2e bonding in carbonium ions is a consequence of the electron deficiency and delocalization associated with the positively charged carbon atoms.^{5,6}

Cremer et al. applied the AIM analysis to study the homoaromaticity of some carbonium ions. They proposed that homoaromatic systems have significant homoconjugative interactions (i.e., interaction indexes reasonably higher than zero).¹⁸ Topological analysis of some simple carbonium ions, such as proponium cations, have been reported.^{18–22} Bader²³ was the first to study the topology of the 2-norbornyl cation. The topological structures of the 2-norbornyl cation and tris-homocyclopropenyl cation also have been studied by Werstiuk et al.^{24–26}

This work aimed to understand the electronic nature of the 3c–2e bonding of the 2-norbornyl cation, its derivative 6,6-

difluoro-2-norbornyl cation, tris-homocyclopropenyl cation, 7-norbornenyl cation, and 4-cyclopentenyl cation and their corresponding silicon analogues. This comparison shows important differences in the electronic nature of the 3c–2e bond of carbonium ions and their corresponding silicon analogues. In addition, the differences of the electronic nature of the 3c–2e bond of the studied carbonium ions also are shown.

Computational Methods

The geometries of the species were optimized by using standard techniques.²⁷ Vibrational analysis on the optimized geometries of selected points on the potential energy surface was performed to determine as to whether the resulting geometries are true minima or transition states by checking the existence of imaginary frequencies. These calculations were performed at the B3LYP/6-311++G** level^{28–31} by using the Gaussian 03 package.³² The electronic density was derived from the Kohn–Sham orbitals obtained at the B3LYP/6-311++G** level and further used for atoms in molecules (AIM) calculations. The critical points, the Laplacian of charge density, the delocalization, and the localization indexes were calculated by means of AIM2000 software.³³

Results and Discussion

All studied systems are depicted in Scheme 1. They were analyzed by AIM theory, which is based on the analysis of the electronic density distribution, $\rho(r)$.^{34,35} In this analysis, an atom in a molecule is rigorously defined as a quantum mechanical entity bound by a three-dimensional surface of zero flux (atomic basin) in the gradient of the electron density. The atomic properties can be obtained by the integration of the electron density within the atomic basin. Then, molecular property is obtained from the summation of the respective atomic property of all the individual atoms of a determined molecule. Much information can be obtained from AIM, such as the bond, cage, and ring critical points (RCP) and their respective eigenvalues (see Supporting Information).

The analysis of the delocalization index (DI) and the Laplacian of the charge density ($\nabla^2\rho(r)$) were used in this work. The DI is a measure of the number of electrons that are shared or exchanged between two atomic basins.^{34,36} It does not measure the delocalization of valence electrons over the whole

* Corresponding authors. E-mail: (C.L.F.) cfirme@iq.ufrj.br and (P.M.E.) pestev@iq.ufrj.br.

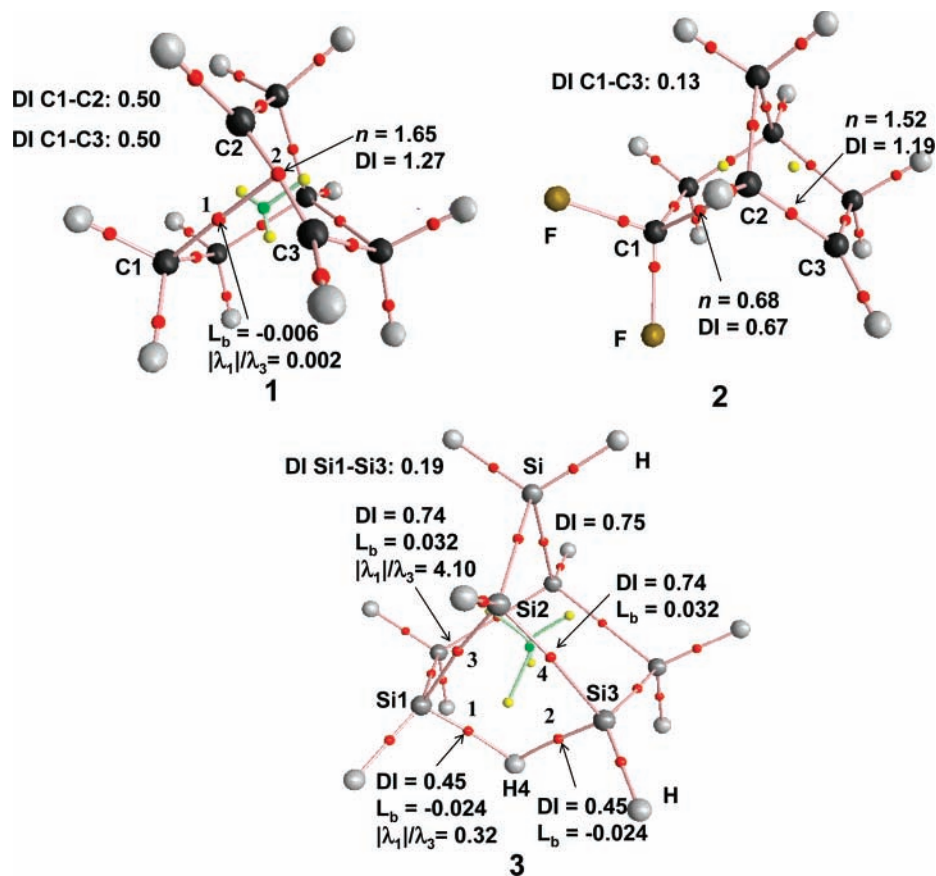
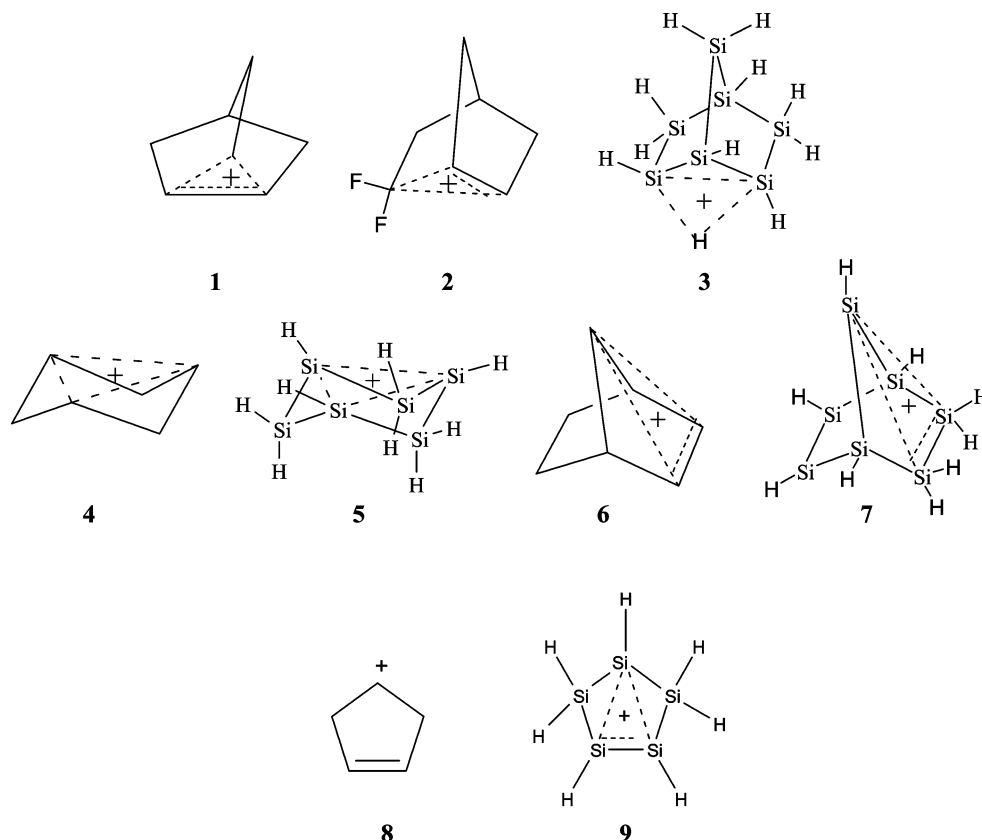


Figure 1. Molecular graphs of cations 1–3. Some DI, values of $|\lambda_1|/\lambda_3$, bond orders (n), and negative Laplacian values (L_b) are also included.

SCHEME 1



molecular system. The $\nabla^2\rho(r)$ value is the sum of the second derivative of the density function at each principal axis (eigenvalues of the Hessian matrix of charge density, λ).^{34,35,37}

The density is locally concentrated in those regions where $L(r) > 0$ and locally depleted in those regions where $L(r) < 0$, where $L(r) = -\nabla^2\rho$. A bond can be characterized by the

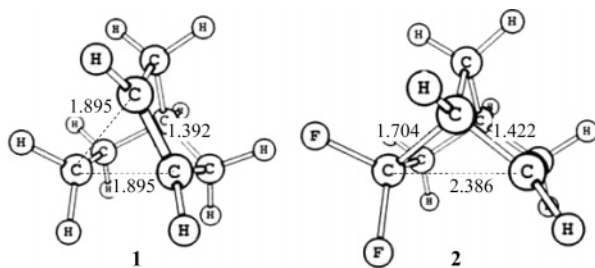


Figure 2. Bond lengths and interatomic distances (Å) involving the 3c–2e bonding system in the cations **1** and **2**.

negative of the Laplacian of the density function at a bond critical point (L_b). If $L_b > 0$, the bond is defined as a shared interaction (covalent bond). In this case, the electronic charge is concentrated in the region between two nuclei. If $L_b < 0$, the bond is defined as a closed-shell interaction (ionic bonds, hydrogen bonds, and van der Waals interactions).³⁸ In addition, in shared interactions, the relation $|\lambda_1/\lambda_3|$ is greater than unity, and in closed-shell interactions, the relation $|\lambda_1/\lambda_3|$ is smaller than 1.³⁴

The existence of a 3c–2e bonding system can be verified by the magnitude of delocalization indexes between atoms of the system. From the studied systems (Scheme 1), the DI of a single C–C bond ranges from 0.93 to 1.00 (see Supporting Information). On the other hand, the DI varies from 0.12 to 0.80 in a 3c–2e bonding system. For $DI < 0.08$, there exists no significant interaction between C–C atoms. In silicon analogues, the DI value ranges from 0.18 to 0.55 in a 3c–2e bonding system. There is a direct relation between delocalization index and bond order (see Supporting Information).

Figure 1 shows the molecular graphs of cations **1**–**3**. All cations follow the Poincaré–Hopf relationship,³⁹ a prerequisite for completeness in the set of critical points of the topology of a given molecular system.

The 2-norbornyl cation **1** has a bond path linking two bond critical points (BCPs 1 and 2) in the 3c–2e system. In cation **2**, the delocalization index between C_1 and C_3 is smaller than that from cation **1** (Figure 1). Probably, the fluorine atoms attract the electronic charge of the C_1 atom.⁴⁰ Hence, the capacity of σ delocalization of the C_1 – C_2 single bond decreases. The AIM theory provides the calculation of the bond order^{18,41} from the relation between bond order (n) and charge density in the BCP

of a C–C bond (ρ_b), $n = \exp[A(\rho_b - B)]$ (see Supporting Information). In Figure 1, one can see that the C_2 – C_3 bond has a bond order much higher than 1 in cations **1** ($n = 1.65$) and **2** ($n = 1.52$). This also shows that σ delocalization in **1** is higher than that from **2** since cation **1** has a higher double character in the C_2 – C_3 bond. From Figures 1 and 2, one can see that cations **1** and **2** have different electronic natures, resulting from different geometrical parameters between them. The bond lengths, the interatomic distances, the delocalization indexes, and the bond order involving all atomic pairs of their corresponding 3c–2e systems are quite different. This influences their topology as well (see Figures 1 and 2).

In cation **3**, the silicon analogue of 2-norbornyl cation **1**, there is a different 3c–2e bonding system (Figure 1). It involves silicon atoms Si_1 and Si_3 and a hydrogen atom. The hydrogen atom is more electronegative than the silicon atom. This affords a different type of 3c–2e bond in cation **3** (Scheme 2).

It is important to note that cation **3** does not form a 4c–2e bonding system because the silicon atom 2 (Si_2) does not participate in this system. The DI values involving Si_1 – Si_2 and Si_2 – Si_3 are typical of single Si–Si bonds ($DI = 0.74$). Moreover, the DI value between Si_2 and H_4 is very low ($DI = 0.08$).

The values of L_b of BCPs 1 and 2 (Figure 1) are negative in cation **3**. The value of the relation $|\lambda_1/\lambda_3|$ from these BCPs is smaller than 1. This means that the interactions involving hydrogen and silicon atoms 1 and 3 are ionic. Moreover, the atomic charge of this hydrogen atom is -0.665 au. Figure 3 shows the contour map of the Laplacian distribution of the charge density of cation **3** in the plane of the 3c–2e system. One can see that there is no overlap of the respective valence shell charge concentration (VSCC) involving hydrogen and silicon atoms 1 and 3. Thus, this hydrogen atom resembles a hydride interacting with two silicon atoms.

In cation **1**, there is no overlap of VSCC between C_1 – C_2 and C_1 – C_3 (Figure 3). This also can be verified by the value of the relation $|\lambda_1/\lambda_3|$ and the value of L_b in the BCP 1 of cation **1** (Figure 1). These results indicate that there is a closed-shell interaction between the C_1 – C_2 and the C_1 – C_3 atomic pairs.

Cation **4** is a C_{3v} symmetric Masamune–Olah homoaromatic species.^{42–44} The reasonable magnitude of delocalization indexes involving carbon atoms 1–3 reveals the existence of a 3c–2e bonding system according to Cremer et al.⁴⁵ There is also a

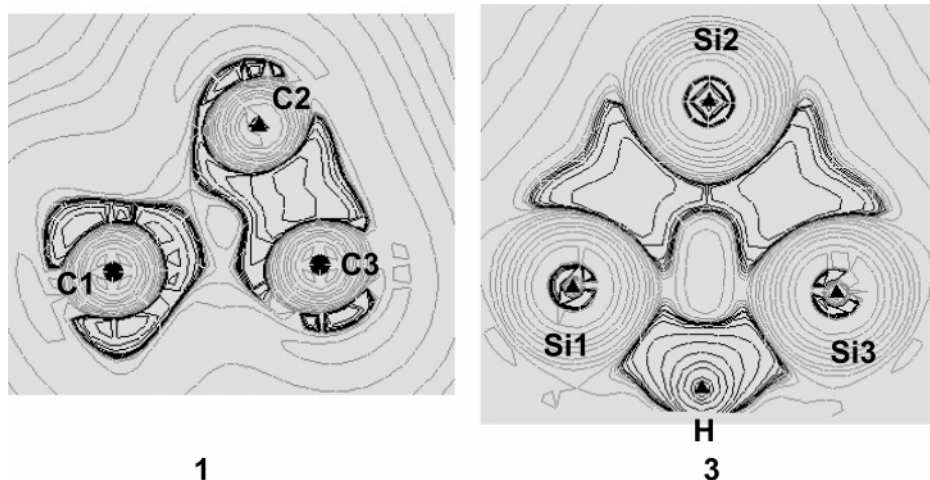


Figure 3. Contour maps of the Laplacian distribution of the electronic charge density of the 3c–2e bonding system of cations **1** and **3**. The gray curves are related to charge depletion, while the black lines are charge concentration.

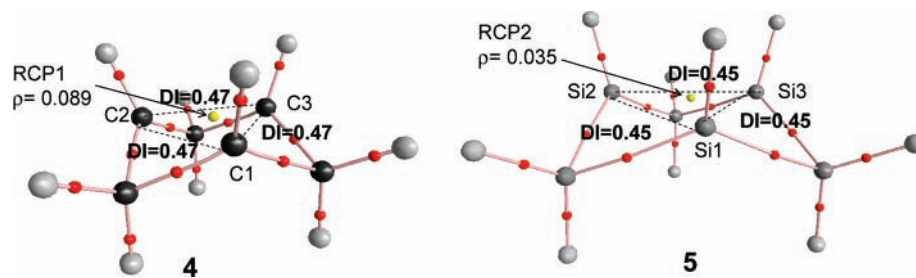


Figure 4. Molecular graphs of cations **4** and **5**, DI involving their respective 3c–2e bonding systems, and charge density (ρ) of their respective RCP in atomic units.

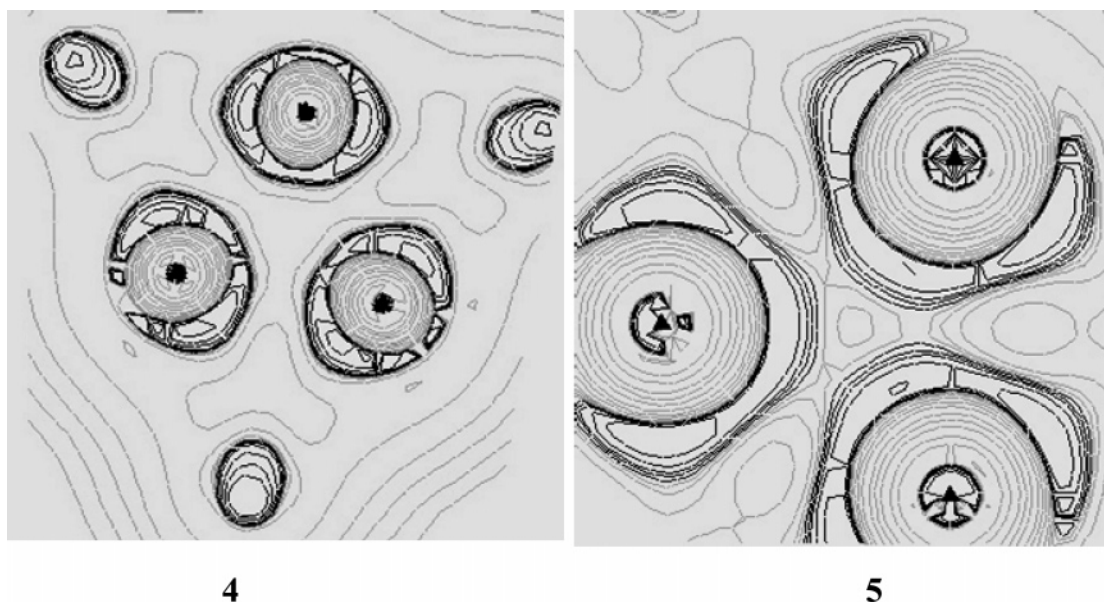
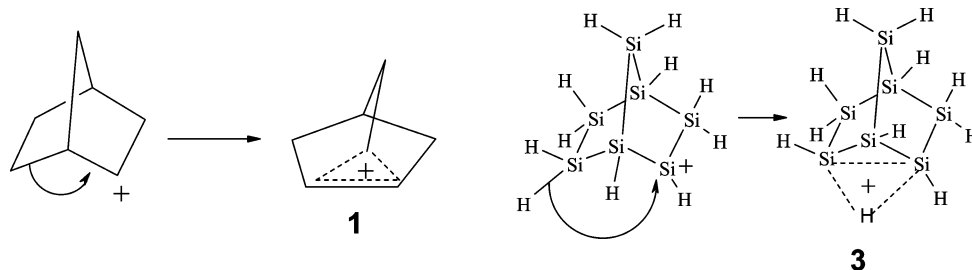


Figure 5. Contour maps of the Laplacian distribution of the electronic charge density of the 3c–2e bonding system of cations **4** and **5**, where the gray curves are related to charge depletion, and the black lines are charge concentration.

SCHEME 2



uniformity of the interaction among them since these DI values are similar (Figure 4).

In cation **5**, the silicon analogue of **4**, it is possible to see the topological similarities between **4** and **5**. The delocalization indexes among $\text{Si}_1\text{--Si}_2\text{--Si}_3$ in **5** and $\text{C}_1\text{--C}_2\text{--C}_3$ in **4** are nearly the same (Figure 4). However, the contour maps of the Laplacian of the electronic charge (Figure 5) of both cations indicate that the distribution of the charge density around $\text{Si}_1\text{--Si}_2\text{--Si}_3$ in cation **5** is less uniform than that in cation **4** since there are more Laplacian lines (gray lines) involving $\text{Si}_1\text{--Si}_2\text{--Si}_3$ atoms in cation **5**. Then, in Figure 4, one can see that the charge density in the RCP of **5** is much smaller than that from cation **4**. Figure 4 also shows that there is no pentacoordinated atom in cations **4** and **5** since no BCP was found between $\text{C}_1\text{--C}_2$, $\text{C}_1\text{--C}_3$, and $\text{C}_3\text{--C}_2$ atomic pairs²⁶ in **4** and between $\text{Si}_1\text{--Si}_2$, $\text{Si}_1\text{--Si}_3$, and $\text{Si}_3\text{--Si}_2$ atomic pairs in **5**.

The delocalization indexes in the 7-norbornenyl cation (**6**) indicate the existence of a 3c–2e bonding system (Figure 6), according to Cremer et al.⁴⁵ The DI values between $\text{C}_2\text{--C}_1$ and $\text{C}_3\text{--C}_1$ are half the delocalization index of a single C–C bond. This means that there is a strong interaction in these atoms. The bond order of the $\text{C}_2\text{--C}_3$ bond ($n = 1.61$) indicates the delocalization of the π electrons within the 3c–2e system. In cation **7**, the silicon analogue of **6**, the delocalization indexes between $\text{Si}_2\text{--Si}_1$ and $\text{Si}_3\text{--Si}_1$ are 73% of a single Si–Si bond. This more effective interaction in cation **7** is related to its small capacity of making double bonds. Then, there is more distribution of the charge density of the π electrons around the Si_1 , Si_2 , and Si_3 atoms. The values of L_b in $\text{Si}_2\text{--Si}_1$ and $\text{Si}_3\text{--Si}_1$ atomic pairs and the corresponding value of the relation $|\lambda_1|/\lambda_3$ indicate that there is a closed-shell interaction between these atomic pairs (Figure 6).

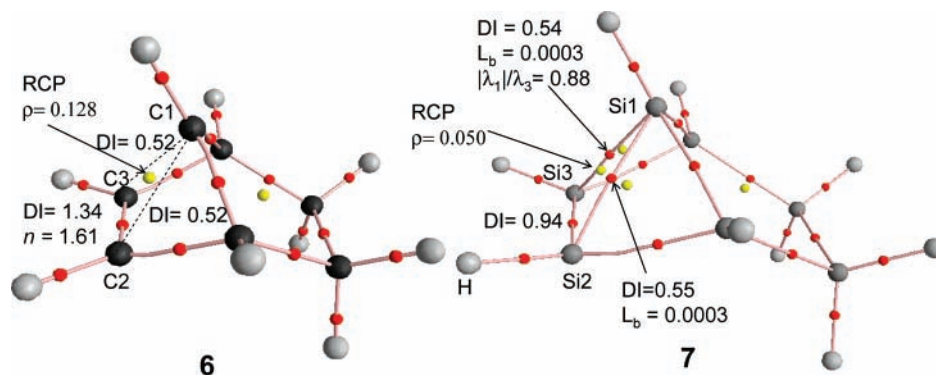


Figure 6. Molecular graphs of the cations **6** and **7**, DI involving their respective $3c-2e$ bonding systems, and charge density (ρ) of their respective RCP in atomic units. Negative of the Laplacian of charge density (L_b), bond order (n), and value of $|\lambda_1/\lambda_3|$ are also included.

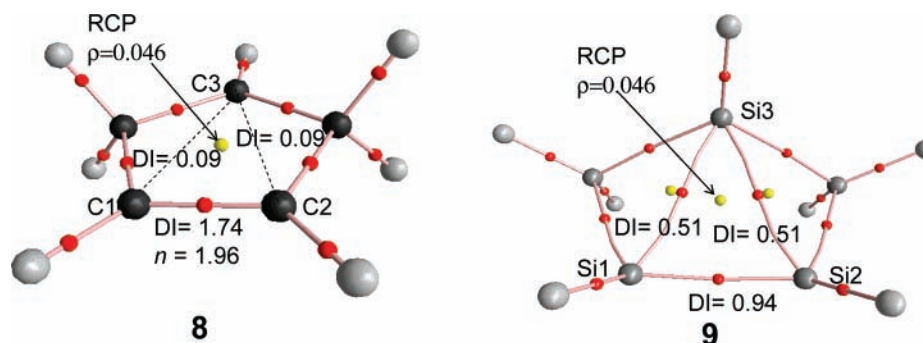


Figure 7. Molecular graphs of cations **8** and **9**, DI involving their respective $3c-2e$ bonding systems, and charge density (ρ) of their respective RCP in atomic units. Bond order (n) is also included.

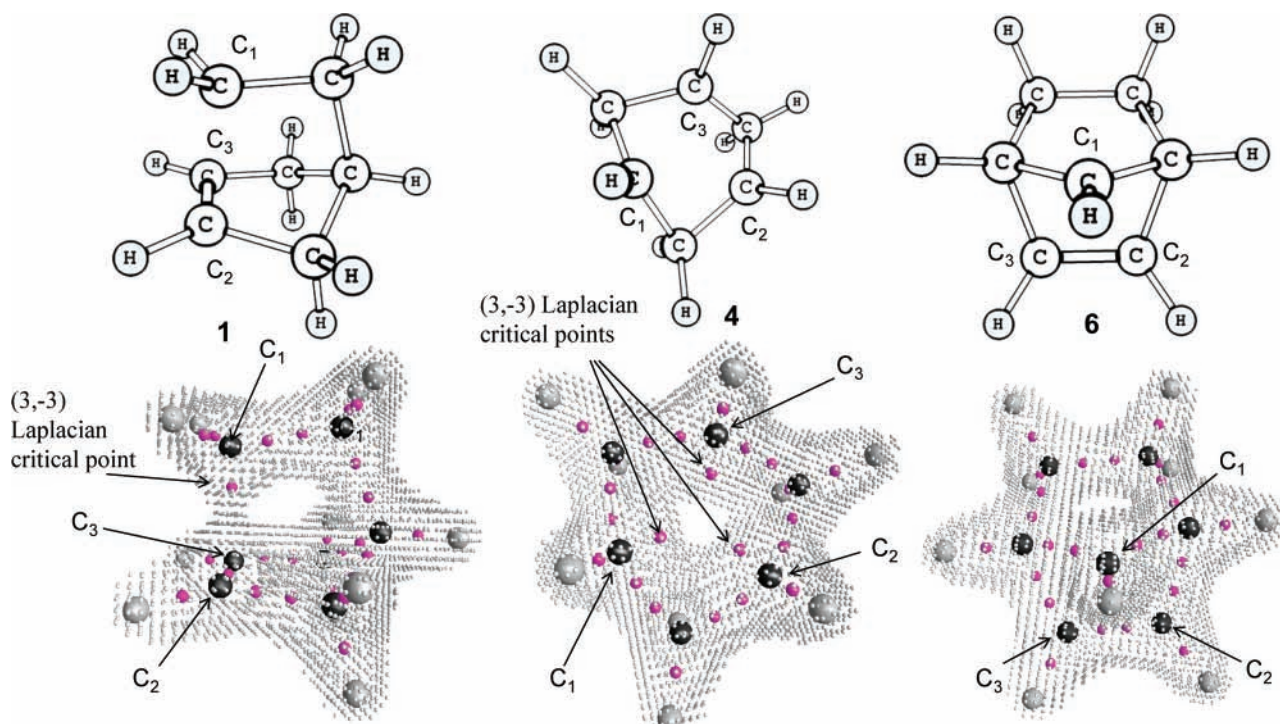


Figure 8. Optimized geometry and corresponding envelope of charge density distribution and $(3,-3)$ critical points of the Laplacian of charge density of cations **1**, **4**, and **6**.

The ellipticity indicates the charge accumulation in the interatomic surface (i.e., the surface that separates two bonding atomic basins). The ellipticities of the bond critical points involving Si_2-Si_1 and Si_3-Si_1 bonds in cation **7** are 4.91. Then, there is a high charge accumulation along the interatomic

surfaces between Si_2-Si_1 and Si_3-Si_1 . The existence of BCPs and their corresponding bond paths, between Si_2-Si_1 and Si_3-Si_1 atomic pairs, does not imply that **7** has stronger homoconjugative interactions than **6**. The L_b value of these critical points is next to zero (Figure 6). Thus, there is no covalent bond

between them. Moreover, the electronic charge distribution in the 3c–2e system of **7** is less uniform than that in **6** because $\rho(3,+1)$ of the 3c–2e system in **7**, with relatively higher DI values, is less than half that from cation **6**.

The cyclopentene cation **8** has a planar geometry and low values of delocalization indexes between C₁–C₃ and C₂–C₃ atom carbons (Figure 7). These results indicate that there is no 3c–2e bonding system in this species. Moreover, the DI and bond order of the C₁–C₂ bond are characteristic of a double bond (Figure 7). The absence of 3c–2e bonding system in **8** is in accordance with Olah et al.'s work that proved that it is a classical ion.⁴⁶ Cation **8** does not have significant homoconjugative interactions (i.e., the DI values involving the methine carbons are close to zero).^{47,48} Thus, cation **8** is not a homoaromatic system as was observed previously.⁴⁰

On the other hand, cation **9**, the silicon analogue of **8**, has significant DI values involving Si₁, Si₂, and Si₃ atoms, and its geometry is not planar. Thus, there exists a 3c–2e bonding system in **9**. Because silicon atoms have a small capacity of making double bonds, the π delocalization is more effective in the cation **9**. Nevertheless, the ellipticities of the BCPs involving Si₁–Si₃ and Si₂–Si₃ bonds are 10.50, which indicate a high concentration of the charge density in the interatomic surfaces between Si₁–Si₃ and Si₂–Si₃. This also indicates the structural instability of these bonds.^{34,35}

Figure 8 shows the optimized geometry and corresponding three-dimensional distribution (envelope) of the charge density. It also depicts the (3,–3) critical points of the Laplacian of the charge density. These values represent a maximum of the charge density concentration in all three curvatures (or coordinates) of the charge density surface.

From Figure 8, one can see that the three-dimensional distribution of the charge density in the region of the 3c–2e system is not the same for every carbonium ion studied in this work. In cation **1**, there is no vacancy in the center of the region of the charge density distribution involving C₁, C₂, and C₃ carbon atoms (in the 3c–2e system). Nonetheless, in **4**, there is a vacancy in the center of the region of the three-dimensional distribution of charge density involving C₁, C₂, and C₃. In **1**, the charge density is not equally distributed throughout the region of the 3c–2e system. Both cations **1** and **4** have a maximum of the charge density concentration or (3,–3) critical points of the Laplacian of the charge density in the region involving their corresponding 3c–2e systems. These are indicated in Figure 8. Instead, in cation **6**, there is no (3,–3) critical points of the Laplacian of the charge density in the region of the 3c–2e system. Thus, cations **1**, **4**, and **6** have topologically different 3c–2e systems, which might give different homoaromatic properties.

Conclusion

The magnitude of all delocalization indexes between atoms of the 3c–2e system can predict homoaromaticity. Cations **1**, **4**, and **6** have topologically different 3c–2e systems.

The electronic nature of the 3c–2e bond in the 2-norbornyl cation (**1**) is different from its difluoro derivative (**2**) and its silicon analogue **3**. In the difluoro derivative (**2**), the interaction among the carbon atoms of the 3c–2e system is smaller than that from the 2-norbornyl cation (**1**). In the silicon analogue **3**, the 3c–2e system involves the interaction of one hydride ion with its vicinal silicon atoms.

The electronic density in the 3c–2e bonding system is more uniform in the 3-bicyclo[3.1.0]hexyl cation (or tris-homocyclopropenyl cation **4**) and in the 7-norbornenyl cation (or bis-

homocyclopropenyl cation **6**) than in their corresponding silicon analogues **5** and **7**. The cyclopentene cation (**8**) does not have homoconjugative interactions, unlike its silicon analogue (**9**).

Acknowledgment. CNPq, CAPES, and FAPERJ are thanked for financial support.

Supporting Information Available: AIM theory, localization and delocalization indexes, bond order in AIM theory, bond order and delocalization index, relation between bond order and charge density, computed energy values of species **1–9**, Z matrices of optimized structures, and total energies and geometry coordinates. This information is available free of charge via the Internet at <http://pubs.acs.org>.

References and Notes

- Olah, G. A.; Bastien, I. J.; Moffatt, M. E.; Kuhn, S. J.; Baker, E. B.; Tolgyesi, W. S. *J. Am. Chem. Soc.* **1963**, *85*, 1328.
- Olah, G. A.; Demember, J. R.; Commeyra, A.; Bribes, J. L. *J. Am. Chem. Soc.* **1971**, *93*, 459.
- Gillespi, R. J. *Acc. Chem. Res.* **1968**, *1*, 202.
- Olah, G. A.; Prakash, G. K. S.; Sommer, J. *Superacids*; Wiley: New York, 1985.
- Olah, G. A.; Prakash, G. K. S. *Carbocation Chemistry*; Wiley: New York, 2004.
- Prakash, G. K. S. *J. Org. Chem.* **2006**, *71*, 3661.
- Winstein, S.; Trifan, D. S. *J. Am. Chem. Soc.* **1949**, *71*, 2953.
- Brown, H. C. *Acc. Chem. Res.* **1973**, *6*, 377.
- Brown, H. C.; Schleyer, P. v. R. *The Nonclassical Ion Problem*; Plenum Press: New York, 1977.
- Olah, G. A. *Acc. Chem. Res.* **1976**, *9*, 41.
- Roberts, J. D.; Mazur, R. H. *J. Am. Chem. Soc.* **1951**, *73*, 3542.
- Johnson, S. A.; Clark, D. T. *J. Am. Chem. Soc.* **1988**, *110*, 4112.
- Olah, G. A.; White, A. M.; Demember, J. R.; Commeyra, A.; Lui, C. Y. *J. Am. Chem. Soc.* **1970**, *92*, 4627.
- Olah, G. A.; Prakash, G. K. S.; Saunders, M. *Acc. Chem. Res.* **1983**, *16*, 440.
- Lipscomb, W. N. *Science (Washington, DC, U.S.)* **1977**, *196*, 1047.
- Kuchitsu, K. *J. Chem. Phys.* **1968**, *49*, 4456.
- Longuet-Higgins, H. C.; Bell, R. P. *J. Chem. Soc.* **1943**, 250.
- Bader, R. F. W.; Slee, T. S.; Cremer, D.; Kraka, E. *J. Am. Chem. Soc.* **1983**, *105*, 5061.
- Okulik, N.; Peruchena, N.; Esteves, P. M.; Mota, C.; Jubert, A. H. *J. Phys. Chem. A* **2000**, *104*, 7586.
- Okulik, N.; Peruchena, N. M.; Esteves, P. M.; Mota, C. J. A.; Jubert, A. *J. Phys. Chem. A* **1999**, *103*, 8491.
- Okulik, N. B.; Peruchena, N. M.; Jubert, A. H. *J. Phys. Chem. A* **2006**, *110*, 9974.
- Okulik, N. B.; Sosa, L. G.; Esteves, P. M.; Mota, C. J. A.; Jubert, A. H.; Peruchena, N. M. *J. Phys. Chem. A* **2002**, *106*, 1584.
- Bader, R. F. W. *Acc. Chem. Res.* **1985**, *18*, 9.
- Werstuijk, N. H.; Muchall, H. M. *J. Mol. Struct.* **1999**, *463*, 225.
- Werstuijk, N. H.; Muchall, H. M. *J. Phys. Chem. A* **2000**, *104*, 2054.
- Werstuijk, N. H.; Wang, Y. G. *J. Phys. Chem. A* **2003**, *107*, 9434.
- Fletcher, R. *Practical Methods of Optimization*; Wiley: New York, 1980; Vol. 1.
- Becke, A. D. *J. Chem. Phys.* **1993**, *98*, 5648.
- Becke, A. D. *J. Chem. Phys.* **1993**, *98*, 1372.
- Lee, C.; Yang, W.; Parr, R. G. *Phys. Rev. B: Condens. Matter Mater. Phys.* **1988**, *37*, 785.
- Dunning, J. T. H. *J. Chem. Phys.* **1989**, *90*, 1007.
- Frisch, M. J.; Trucks, G. W.; Schlegel, H. B.; Scuseria, G. E.; Robb, M. A.; Cheeseman, J. R.; Zakrzewski, V. G.; Montgomery, J. A., Jr.; Vreven, T.; Kudin, K. N.; Burant, J. C.; Millam, J. M.; Iyengar, S. S.; Tomasi, J.; Barone, V.; Mennucci, B.; Cossi, M.; Scalmani, G.; Rega, N.; Petersson, G. A.; Nakatsuji, H.; Hada, M.; Ehara, M.; Toyota, K.; Fukuda, R.; Hasegawa, J.; Ishida, M.; Nakajima, T.; Honda, Y.; Kitao, O.; Nakai, H.; Klene, M.; Li, X.; Knox, J. E.; Hratchian, H. P.; Cross, J. B.; Adamo, C.; Jaramillo, J.; Gomperts, R.; Stratmann, R. E.; Yazyev, O.; Austin, A. J.; Cammi, R.; Pomelli, C.; Ochterski, J. W.; Ayala, P. Y.; Morokuma, K.; Voth, G. A.; Salvador, P.; Dannenberg, J. J.; Zakrzewski, V. G.; Dapprich, S.; Daniels, A. D.; Strain, M. C.; Farkas, O.; Malick, D. K.; Rabuck, A. D.; Raghavachari, K.; Foresman, J. B.; Ortiz, J. V.; Cui, Q.; Baboul, A. G.; Clifford, S.; Cioslowski, J.; Stefanov, B. B.; Liu, G.; Liashenko, A.; Piskorz, P.; Komaromi, I.; Martin, R. L.; Fox, D. J.; Keith, T.; Al-Laham, M. A.; Peng, C. Y.; Nanayakkara, A.; Challacombe, M.; Gill, P. M. W.; Johnson, B.; Chen, W.; Wong, M. W.; Gonzalez, C.; Pople, J. A.; *Gaussian 03*; Gaussian, Inc.: Pittsburgh, PA, 2003.

- (33) Biegler-König, F.; Schönbohm, J. *AIM2000*, version 2.0; Büro Streibel Biegler-König, 2002.
- (34) Bader, R. F. W. *Atoms in Molecules: A Quantum Theory*, 1st ed.; Oxford Press: Oxford, 1994.
- (35) Popelier, P. L. A. *Atoms in Molecules: An Introduction*, 1st ed.; Prentice Hall: Manchester, U.K., 2000.
- (36) Bader, R. F. W.; Streitwieser, A.; Neuhaus, A.; Laidig, K. E.; Speers, P. *J. Am. Chem. Soc.* **1996**, *118*, 4959.
- (37) Popelier, P. L. A. *Coord. Chem. Rev.* **2000**, *197*, 169.
- (38) Gibbs, G. V.; Spackman, M. A.; Jayatilaka, D.; Rosso, K. M.; Cox, D. F. *J. Phys. Chem. A* **2006**, *110*, 12259.
- (39) Balanarayan, P.; Gadre, S. R. *J. Chem. Phys.* **2003**, *119*, 5037.
- (40) Szabo, K. J.; Kraka, E.; Cremer, D. *J. Org. Chem.* **1996**, *61*, 2783.
- (41) Bader, R. F. W.; Tang, T. H.; Tal, Y.; Bieglerkonig, F. W. *J. Am. Chem. Soc.* **1982**, *104*, 946.
- (42) Olah, G. A.; Prakash, G. K. S.; Rawdah, T. N.; Whittaker, D.; Rees, J. C. *J. Am. Chem. Soc.* **1979**, *101*, 3935.
- (43) Prakash, G. K. S.; Arvanaghi, M.; Olah, G. A. *J. Am. Chem. Soc.* **1985**, *107*, 6017.
- (44) Winstein, S.; Sonnenberg, J. *J. Am. Chem. Soc.* **1961**, *83*, 3235.
- (45) Cremer, D.; Kraka, E.; Slee, T. S.; Bader, R. F. W.; Lau, C. D. H.; Nguyendang, T. T.; Macdougall, P. J. *J. Am. Chem. Soc.* **1983**, *105*, 5069.
- (46) Olah, G. A.; Berrier, A. L.; Arvanaghi, M.; Prakash, G. K. S. *J. Am. Chem. Soc.* **1981**, *103*, 1122.
- (47) Childs, R. F.; Cremer, D.; Elia, G. *The Chemistry of the Cyclopropyl Group*; J. Wiley and Sons: Chichester, U.K., 1995; Vol. 2.
- (48) Williams, R. V. *Chem. Rev.* **2001**, *101*, 1185.